

Research Paper Series

No. 66

On the Environmental Kuznets Curve: An Real Options Approach

Masaaki Kijima[†], Katsumasa Nishide[‡] and Atsuyuki Ohyama[§]

September, 2009

[†] Graduate School of Social Sciences, Tokyo Metropolitan University

[‡] Interdisciplinary Research Center, Yokohama National University

[§] Financial Research Group, NLI Research Institute

On the Environmental Kuznets Curve: A Real Options Approach*

Masaaki Kijima^{a†}, Katsumasa Nishide^b and Atsuyuki Ohyama^c

a *Graduate School of Social Sciences, Tokyo Metropolitan University.*

b *Interdisciplinary Research Center, Yokohama National University.*

c *Financial Research Group, NLI Research Institute.*

(August 10, 2009)

Abstract. Previous researches have suggested that some pollutant levels first increases due to the economic growth and then starts decreasing, the pattern being called the ‘environmental Kuznets curve’. Assuming that each policy maker optimally executes the switching options of regulation and deregulation for pollution, the switching dynamics of environmental policy is described by an alternating renewal process. It is shown that the double Laplace transform of transition density of a pollutant level can be obtained by a novel application of renewal theory. The expected level of overall pollutants is then calculated numerically and found to exhibit either a Λ -shaped or an N -shaped pattern in time. Our results present a simple explanation for the environmental Kuznets curve within a real options framework.

Keywords: Environmental Kuznets curve, real option, alternating renewal process, double Laplace transform.

JEL classification: Q52; G11, Q58

* The second author greatly appreciates the financial support by the Japanese Ministry of Education, Science, Sports, and Culture (MEXT), “Special Coordination Funds for Promoting Science and Technology”.

† Corresponding author: Graduate School of Social Sciences, Tokyo Metropolitan University, 1-1 Minami-Ohsawa, Hachiohji, Tokyo 192-0397, Japan. TEL:+81-42-677-2330, FAX:+81-42-677-2298, E-mail: kijima@tmu.ac.jp

1 Introduction

The issue of worldwide environment has drawn attention, since the global warming and other environmental problems are becoming more and more serious. In particular, it is an urgent subject for all authorities who are responsible for environmental policies to understand and predict how the environmental quality will evolve over time.

The environmental Kuznets curve (EKC for short) is referred to as the hypothesis that the relation between the pollution and per capita income exhibits an inverse-U shape. More specifically, the pollution level rapidly increases at an initial stage of economic development, and then starts decreasing as the economy becomes developed and mature.¹

Since early 1990s, heated debates have been made on the EKC. A plenty of empirical studies support the inverted-U relationship of the pollution level with respect to per capita income, although some other papers are skeptical about the hypothesis. For example, Grossman and Krueger (1995) reported that some toxic gas pollution has an inverted-U relationship with per capita income, while Arrow et al. (1995) cast doubt on the hypothesis. In addition, some papers have found that the relation is not of an inverse-U shape, but of an N shape, meaning that the environmental degradation starts increasing again after a decrease to a certain level (e.g., de Bruyn and Opschoor, 1997; Sengupta, 1997).

In contrast to the vast empirical literature on the EKC, there are only a few theoretical studies to explain why the EKC appears. Moreover, in the theoretical literature, most studies mainly focus on the macroeconomic production and/or the utility of a representative agent, where the production and utility functions are assumed to depend on some environmental quality. For example, among others, Lopez (1994), Jones and Manuelli (2000) and Brock and Taylor (2004) consider a macroeconomic production function in a dynamic setting, and analyze an optimal path of pollution level. Other papers such as Selden and Song (1995), Stokey (1998) and Andreoni and Levinson (2001) investigate how the functional form of the utility affects the dynamics of environmental degradation. Note that the existing theoretical papers illustrate only an inverse-U shape, and none of them show an N -shaped EKC pattern. See a companion paper Kijima et al. (2009) for an overall survey of the EKC literature.

There are no studies, to the authors' best knowledge, that examine the evolution of pollution as the aggregation of microeconomic behaviors. As Arrow et al. (1995) pointed out, the relation should be shown to be valid for the accumulation of stocks of waste or for pollutants involving long term and more dispersed costs. This paper first builds a model

¹ Originally, Kuznets (1955) suggested that, as per capita income increases, income inequality also increases at first but then, after some turning point, starts declining.

from a microeconomic point of view and then describes how an aggregated pollution level evolves over a long period of time.

Moreover, none of the above models include uncertainty in the economy, and the dynamics of environmental quality (and also per capita income) is assumed to be deterministic. Pindyck (2006) emphasizes that a study of an environmental problem should capture the following three characteristics; (i) uncertainties in future costs and benefits resulting from an environmental policy, (ii) time irreversibility of a policy owing to sunk costs, and (iii) a timing option in adopting a policy.

A real options approach is a useful tool to study the dynamics of environmental quality under an economy with uncertainty. There are many papers that theoretically study environmental issues in this framework (e.g., Pindyck, 2000, 2002; Wirl, 2006). Also, its empirical application has attracted much attention (e.g., Michailidis and Mattas, 2007; Nishide and Ohyama, 2009).

This paper considers the problem of how *overall* environmental quality evolves over time when *each* local authority optimally executes his/her policy under uncertainty. To this end, we follow the spirit of Wirl (2006) and consider the problem within a real options framework. In Wirl (2006), an economic agent faces the problem of which action to take; production with pollution or suspension of pollution, and it is shown that there are two thresholds in pollution level for the policy to switch the two actions. In our model, each policy maker chooses one of two alternatives; deregulation or tight regulation for the environment.

Our analysis consists of two steps. First, we set up our model as a problem of an individual policy maker. It will be shown that, when each local authority optimally adopts the policy, there exist two thresholds in pollution level to switch the two policies as in Wirl (2006); the upper threshold to shift from deregulation to regulation and the lower threshold from regulation to deregulation. Consequently, the switching dynamics of the environmental policy follows the so-called *alternating renewal process*. Based on the theory of renewal processes, the transition probability density of the pollution level can be calculated via a double Laplace transform technique.

Second, we consider the accumulation of pollution levels for all local areas, and study the evolution of the aggregated pollution in time. When there are many local authorities and their environmental policies are executed independently, thanks to the weak law of large numbers, the aggregated level of pollutions can be approximated as the weighted average of the expected pollution levels. The expected level of overall pollutants is calculated numerically by using the inverse Laplace transform.

This paper provides a theoretical framework to explain why the EKC presents in the

aggregated level of pollutants from the viewpoint of policy effects.² Namely, each policy maker has two alternative policies, tight regulation and deregulation, for the environment. Tight regulation reduces disutility caused by the pollution, while deregulation brings higher benefits of economic activities.

When each policy maker optimally executes the environmental policy under the trade-off, the aggregated level of pollution exhibits an EKC pattern in a fairly general setting, without explicitly considering economic growth and/or utility. This means that an environmental policy switch by each policy maker is an important factor for the dynamics of overall pollutions, and the EKC is a result from environmental policy executions in the aggregated level.

The advantage of our model is that it can produce not only a hump shape (hereafter we call it a Λ shape) but also an N shape for the aggregated pollution level, as reported in some empirical works. Recall that the previous theoretical papers explain only a hump-shaped pattern, implying that environmental degradation never increases again once it starts decreasing at some level, unless per capita income decreases. Our model is flexible enough to demonstrate the both curves. The main contribution of this paper is to show that the aggregated level of pollutants naturally exhibits various shapes, including Λ and N shapes, due to environmental policy switches of individual policy makers.

The rest of this paper is organized as follows. In the next section, we describe our model and derive the optimal environmental policy for a policy maker of each local area. The policy is determined by two thresholds of pollution level for regulation and deregulation. Section 3 analyzes the stochastic behavior of the pollutant level in each local area and derives its transition density function. In Section 4, we consider the accumulation of pollutant levels in all local areas, and study the evolution in time of the aggregated pollution level. The *double* Laplace transform of the transition density function of the pollutant level with respect to both time and state is obtained by a novel application of the renewal theory. The expected level of overall pollutants is then inverted back numerically, using the derivative of the double Laplace transform with respect to state, and found to exhibit either a Λ -shaped or an N -shaped patterns in time, depending on the parameter setting. This result sheds a new light on how overall environmental quality evolves in time. Section 5 concludes this paper. Explicit formulas of the Laplace transforms of interest and the proofs of propositions are given in Appendix.

² There is an argument that the evolution of pollution is linked not only with a development path or economic growth, but also with policy response. See, e.g., Grossman and Krueger (1995); Magnani (2001).

2 The Optimal Environmental Policy

In this section, we describe our model and solve the optimal environmental policy of a *local* authority from the viewpoint of individual policy maker. Our model is similar to Wirl (2006), although there are some important differences.

Suppose that each policy maker faces the problem of which policy to take for an environmental pollution; tight regulation or deregulation. When the policy maker adopts the regulation, the level of the pollution can be reduced in the local area with other economic benefits being given up. On the other hand, when he/she chooses the deregulation policy, the area enjoys higher economic benefits, while a higher cost or disutility is incurred due to the pollution. The policy maker can shift the policy to the other at any time; but a fixed and irreversible cost is required for the policy switch.

2.1 The model

Suppose that a policy maker faces an environmental policy problem in a local area, where the local area could be a country, a province, a city or another type of authority that is responsible for environmental policies. The policy maker can choose one of two alternative policies: tight regulation or deregulation. For notational convenience, we denote the states of regulation and deregulation policies by L and H , respectively.

Let S_{it} represent the policy state of local area i at time t , and assume that, when $S_{it} = k$, $k = L, H$, the level of pollution, P_{it} , evolves according to the process

$$dP_{it} = \alpha_{ik}P_{it}dt + \sigma_{ik}P_{it}dz_t^i, \quad S_{it} = k, \quad (2.1)$$

where z_t^i is a standard Brownian motion and α_{ik} and σ_{ik} are some constants. That is, the process of the pollution level follows a geometric Brownian motion (GBM hereafter) whose drift and volatility coefficients vary over time, depending on the state of the selected policy. It is plausible to assume that $\alpha_{iH} > \alpha_{iL}$ and $\sigma_{iH} \geq \sigma_{iL}$, because deregulation policy induces a higher and more volatile level of pollution.

The pollution incurs negative effects on the economy of the local area. We assume that the disutility of the pollution is proportional to the level of pollution P on the monetary base and is given by

$$C_i(P) = c_iP,$$

where c_i is a positive constant that represents the magnitude of the effect on the economy of local area i .

Table 1: The structure of our model.

	Drift	Volatility	Benefit	Switching cost
Deregulation ($S_i = H$)	α_{iH}	σ_{iH}	u_{iH}	K_{iH} ($H \rightarrow L$)
Regulation ($S_i = L$)	α_{iL}	σ_{iL}	u_{iL}	K_{iL} ($L \rightarrow H$)
Relation	$\alpha_{iH} > \alpha_{iL}$	$\sigma_{iH} \geq \sigma_{iL}$	$u_{iH} > u_{iL}$	$K_{iH} > K_{iL}$

At this point, we remark the differences between our model and that of Wirl (2006). In Wirl (2006), the level of environmental degradation P_{it} is assumed to follow an Ornstein–Uhlenbeck (OU) process, and the cost function is quadratic. Hence, in his setting, P_{it} can become negative with strictly positive probability, and disutility accrues from negative pollutants. On the other hand, in our model, the level of pollution P_{it} follows a GBM, which always takes positive values, when the policy state S_{it} is given. Also the disutility is monotonic in the level of pollution. Therefore, our setting seems more realistic when the optimal policy for environmental regulations is considered.

If the effect from environmental pollution is not taken into account, deregulation policy usually brings higher economic benefits to each local area, thanks to free and active businesses. On the other hand, when the policy imposes tight regulation for the environment, its economic activities can be shrunk, resulting in a negative effect on the economy. We represent the benefits of local area i from deregulation and tight regulation by u_{iH} and u_{iL} , respectively. Of course, it is assumed that $u_{iH} > u_{iL}$.

Finally, as in Wirl (2006), the shift of the policy is assumed to accompany an irreversible cost. The switching cost from deregulation (H) to tight regulation (L) is given by K_{iH} , while the cost of the switch from L to H is K_{iL} . It is assumed that $K_{iH} > K_{iL}$, because the policy change to tight regulation is more difficult to implement, whence being more costly. Table 1 summarizes the structure of our model.

In our setting, the policy maker faces a trade-off between the benefit u_{ik} of free business activities and disutility $c_i P_i$ caused by the pollution. That is, when the policy is in state H , the local area enjoys a higher level of economic benefits u_{iH} , although the level of pollution may grow rapidly on average, causing a negative effect on the economy. On the other hand, when the policy is in state L , the pollution level may be decreasing at the sacrifice of economic growth.

Suppose that $S_{i0} = H$,³ and define the sequences of time epochs, denoted by T_{Hn}^i and

³ Throughout the paper, we assume that $S_{i0} = H$, unless stated otherwise. The results for the case that

T_{Ln}^i , to switch the policy recursively by

$$\begin{cases} T_{Hn}^i \equiv \inf\{t \geq T_{L,n-1}^i : S_{it} = L\}, \\ T_{Ln}^i \equiv \inf\{t \geq T_{Hn}^i : S_{it} = H\}, \end{cases} \quad n = 1, 2, \dots,$$

with $T_{L0}^i = 0$. Formally, the maximization problem of the policy maker is described as

$$\sup_{\{T_{Hn}^i, T_{Ln}^i\}_n} E \left[\sum_{k=H,L} \left\{ \int_0^\infty e^{-rt} 1_{\{S_{it}=k\}} (u_{ik} - c_i P_{it}) dt - \sum_n e^{-rT_{kn}^i} K_{ik} \right\} \middle| P_{i0} \right], \quad (2.2)$$

where r is the instantaneous discount factor and 1_A denotes the indicator function, i.e. $1_A = 1$ if A is true and $1_A = 0$ otherwise. Here, it is assumed that $r > \alpha_{ik}$, $k = H, L$, to ensure the existence of (2.2).

A standard argument in the real options literature yields the optimal policy for the problem (2.2) as follows. Let us denote the value function of local area i at state k by $V_{ik} = V_{ik}(P_i)$. Then, the value function satisfies the second-order ordinary differential equation (ODE for short)

$$\frac{\sigma_{ik}^2}{2} P_i^2 V_{ik}''(P_i) + \alpha_{ik} P_i V_{ik}'(P_i) - r V_{ik}(P_i) + u_{ik} - c_i P_i = 0, \quad k = H, L. \quad (2.3)$$

The value function can be solved as

$$V_{ik}(P_i) = A_{ik} P_i^{\beta_{ik}} + \frac{u_{ik}}{r} - \frac{c_i P_i}{r - \alpha_{ik}}, \quad k = H, L, \quad (2.4)$$

where A_{ik} is some constant (obtained below) and β_{ik} is a (negative for $k = H$ and positive for $k = L$) root of the characteristic function of the ODE (2.3), i.e.,

$$\beta_{iH} \equiv \frac{1}{2} - \frac{\alpha_{iH}}{\sigma_{iH}^2} - \sqrt{\left(\frac{1}{2} - \frac{\alpha_{iH}}{\sigma_{iH}^2}\right)^2 + \frac{2r}{\sigma_{iH}^2}} < 0$$

and

$$\beta_{iL} \equiv \frac{1}{2} - \frac{\alpha_{iL}}{\sigma_{iL}^2} + \sqrt{\left(\frac{1}{2} - \frac{\alpha_{iL}}{\sigma_{iL}^2}\right)^2 + \frac{2r}{\sigma_{iL}^2}} > 0.$$

The optimal environmental policy in this setting is represented by the following rule. When the current policy is deregulation, the policy maker optimally changes its policy to tight regulation at the time that the process P_{it} first reaches an upper threshold \bar{P}_i . Similarly, when the current policy is tight regulation, there is a lower threshold \underline{P}_i , $\underline{P}_i < \bar{P}_i$, at which the policy switches to deregulation. That is, the time epochs at which policy changes occur are given recursively by

$$\begin{cases} T_{Hn}^i = \inf\{t \geq T_{L,n-1}^i : P_{it} \geq \bar{P}_i\}, \\ T_{Ln}^i = \inf\{t \geq T_{Hn}^i : P_{it} \leq \underline{P}_i\}, \end{cases} \quad n = 1, 2, \dots,$$

$S_{i0} = L$ are provided in Appendix A.4.

Table 2: The base case parameters for comparative statics on the thresholds.

	r	c	u_k	α_k	σ_k	K
L	0.05	5	100	-0.004	0.055	200
H	0.05	5	0	0.043	0.025	20

with $T_{L0} = 0$.

Note that there are four unknown parameters A_{iH} , A_{iL} , \bar{P}_i and \underline{P}_i , which can be determined by the value-matching conditions

$$V_{iH}(\bar{P}_i) = V_{iL}(\bar{P}_i) - K_{iH}, \quad V_{iL}(\underline{P}_i) = V_{iH}(\underline{P}_i) - K_{iL}$$

and the smooth-pasting conditions

$$V'_{iH}(\bar{P}_i) = V'_{iL}(\bar{P}_i), \quad V'_{iL}(\underline{P}_i) = V'_{iH}(\underline{P}_i).$$

Since there are four equations for the four unknown parameters, the value functions $V_{ik}(P_i)$, $k = H, L$, given by (2.4) and the thresholds \bar{P}_i , \underline{P}_i are obtained simultaneously at least numerically.

2.2 Comparative statics

In this subsection, we provide comparative statics results to show the impact of each parameter on the thresholds \bar{P}_i , \underline{P}_i through numerical examples. The base case parameters are presented in Table 2.⁴ Figure 1 describes how some of the parameters affect the thresholds for policy switches.

[Figure 1 is inserted here]

All of these effects in Figure 1 are consistent with the standard real options theory. For example, consider the case that the switching cost K_{iH} to tight regulation from deregulation is large. In this case, when $S_{it} = H$, the policy maker of local area i is unwilling to switch the policy from deregulation to regulation due to the high irreversible cost, resulting in a higher upper threshold \bar{P}_i . Then, the first term of (2.4) with $k = H$, the option value of V_{iH} , becomes smaller. On the other hand, when local area i is in the regulation state ($S_{it} = L$), the policy maker knows that the policy switch does not easily happen once deregulation

⁴ Some of the parameters are consistent with those in Table 4 of Section 4.2, which are estimated from actual data.

policy is adopted. This means that the option value of V_{iL} (the first term of (2.4) with $k = L$) also becomes smaller, and the policy maker has less incentive to change the policy from regulation to deregulation, resulting in a smaller lower threshold \underline{P}_i . This explains why a higher K_{iH} widens the upper and lower thresholds as observed in Figure 1 (a).

For intuitive explanations on the other results, we refer to a standard textbook such as Dixit and Pindyck (1994).

3 Stochastic Behavior of the Pollutant Level

In the previous section, we show that each policy maker follows the so-called on-off switching strategy, where ‘on’ stands for L (regulation) and ‘off’ for H (deregulation), to maximize the expected total (discounted) profit. In this section, given the strategy, we analyze the stochastic behavior of the pollutant level of each local area. The key idea for this purpose is to recall that the policy switching follows an *alternating renewal process*.⁵

Here and hereafter, we investigate the evolution of $x_{it} \equiv \log P_{it}$ rather than P_{it} itself, because x_{it} is easier to handle mathematically. It is readily seen from Ito’s formula that, given $S_{it} = k$, $k = H, L$, x_t follows an arithmetic Brownian motion, because

$$dx_{it} = \mu_{ik}dt + \sigma_{ik}dz_t^i, \quad k = H, L, \quad (3.1)$$

where $\mu_{ik} \equiv \alpha_{ik} - \sigma_{ik}^2/2$. Similarly, we define the thresholds $\bar{x}_i = \log \bar{P}_i$ and $\underline{x}_i \equiv \log \underline{P}_i$. The stopping times for policy switches are expressed recursively as

$$\begin{cases} T_{Hn}^i = \inf\{t \geq T_{L,n-1}^i : x_{it} \geq \bar{x}_i\}, \\ T_{Ln}^i = \inf\{t \geq T_{Hn}^i : x_{it} \leq \underline{x}_i\}, \end{cases} \quad n = 1, 2, \dots, \quad (3.2)$$

with $T_{L0}^i = 0$. Throughout this section, we assume that $x_{i0} < \bar{x}_i$, so that $S_{i0} = H$. See Appendix A.4 for the results when $S_{i0} = L$.

In the rest of this section, we suppress the script i for notational simplicity, unless confusions occur.

3.1 Alternating renewal processes

For the stopping times given by (3.2), we define the *interarrival times* recursively by

$$\begin{cases} \tau_{Hn} \equiv T_{Hn} - T_{L,n-1}, \\ \tau_{Ln} \equiv T_{Ln} - T_{Hn}, \end{cases} \quad n = 1, 2, \dots$$

⁵ See, e.g., standard textbooks such as Kijima (1997) and Ross (1983) for details of alternating renewal processes.

Table 3: Density functions of interarrival time.

Interarrival time	Density function
τ_{H1}	$f_{0H}(t)$
$\tau_{Ln}; n = 1, 2, \dots$	$f_L(t)$
$\tau_{Hn}; n = 2, 3, \dots$	$f_H(t)$

Due to the strong Markov property of Brownian motions, all the interarrival times are mutually independent. Also, because the process x_t is homogeneous in time, $\{\tau_{Ln}\}_{n=1}^{\infty}$ and $\{\tau_{Hn}\}_{n=2}^{\infty}$ are sequences of IID (independent, identically distributed) random variables. Note that τ_{H1} may follow a different distribution from τ_{Hn} , $n \geq 2$, because the initial state x_0 may differ from \underline{x} (note that $\underline{x} < \bar{x}$). The density functions of interarrival times are denoted as in Table 3.

The interarrival times are the first hitting times of Brownian motion x_t . For example, τ_{Ln} is the first hitting time of x_t to the lower threshold \underline{x} starting from \bar{x} . Hence, from the standard argument of first hitting times of Brownian motions, we obtain

$$f_{0H}(t) = \frac{\bar{x} - x_0}{\sigma_H \sqrt{2\pi t^3}} \exp \left\{ -\frac{(\bar{x} - x_0 - \mu_H t)^2}{2\sigma_H^2 t} \right\}, \quad (3.3)$$

$$f_L(t) = \frac{\bar{x} - \underline{x}}{\sigma_L \sqrt{2\pi t^3}} \exp \left\{ -\frac{(\bar{x} - \underline{x} + \mu_L t)^2}{2\sigma_L^2 t} \right\} \quad (3.4)$$

and

$$f_H(t) = \frac{\bar{x} - \underline{x}}{\sigma_H \sqrt{2\pi t^3}} \exp \left\{ -\frac{(\bar{x} - \underline{x} - \mu_H t)^2}{2\sigma_H^2 t} \right\}. \quad (3.5)$$

For notational convenience, we introduce the *convolution* operator. For two density functions $f(t)$ and $g(t)$, their convolution is defined by

$$f * g(t) \equiv \int_0^t f(u)g(t-u)du, \quad t \geq 0.$$

Also, the Laplace transform of function $f(t)$ with respect to t is denoted by

$$\mathcal{L}_t[f](\theta) \equiv \int_0^{\infty} e^{-\theta t} f(t) dt$$

for which the integral exists. It is well known that

$$\mathcal{L}_t[f * g](\theta) = \mathcal{L}_t[f](\theta)\mathcal{L}_t[g](\theta) \quad (3.6)$$

for which the integrals exist.

Now, let $N_k(t)$, $k = H, L$, be the number of times that the policy maker switches its policy to state k until time t , i.e.,

$$N_k(t) \equiv \max\{n : T_{kn} \leq t\}, \quad t \geq 0, \quad k = H, L.$$

Since $\{\tau_{Ln}\}_{n=1}^{\infty}$ and $\{\tau_{Hn}\}_{n=2}^{\infty}$ are IID sequences, the stochastic processes $N_k(t)$, $k = H, L$, form (delayed) alternating renewal processes. The respective renewal functions are defined as

$$M_k(t) \equiv E[N_k(t)], \quad t \geq 0, \quad k = H, L,$$

and the associated renewal densities are given by

$$m_k(t) \equiv \frac{d}{dt}E[N_k(t)], \quad t > 0, \quad k = H, L.$$

By the definition of renewal densities, since no multiple jumps occur during the infinitesimal time interval $(t, t + dt]$, we informally express

$$m_k(t)dt = E[N_k(t + dt) - N_k(t)] = P\{N_k(t + dt) - N_k(t) = 1\},$$

whence we obtain

$$m_k(t)dt = P\{\text{policy switch to state } k \text{ occurs in } (t, t + dt]\}, \quad t \geq 0, \quad k = H, L. \quad (3.7)$$

This is the key observation in the following analysis.

For renewal processes, it is well known that the Laplace transforms of the interarrival densities play a key role. We follow the standard argument of the basic renewal theory to show that the renewal densities are given by

$$m_H(t) = f_{0H}(t) + m_H * f_L * f_H(t), \quad t \geq 0,$$

and

$$m_L(t) = f_{0L}(t) + m_L * f_H * f_L(t), \quad t \geq 0.$$

Then, operating the Laplace transform to the above expressions, we obtain from (3.6) that

$$\mathcal{L}_t[m_H](\theta) = \frac{\mathcal{L}_t[f_{0H}](\theta)}{1 - \mathcal{L}_t[f_L](\theta)\mathcal{L}_t[f_H](\theta)} \quad (3.8)$$

and

$$\mathcal{L}_t[m_L](\theta) = \frac{\mathcal{L}_t[f_{0L}](\theta)\mathcal{L}_t[f_L](\theta)}{1 - \mathcal{L}_t[f_L](\theta)\mathcal{L}_t[f_H](\theta)}, \quad (3.9)$$

respectively. The explicit formulas of the Laplace transforms $\mathcal{L}_t[m_H](\theta)$ and $\mathcal{L}_t[m_L](\theta)$ are given by (A.1) and (A.2), respectively, in Appendix A.1. The renewal densities $m_k(t)$, $k = H, L$, can then be obtained via the inverse Laplace transform.

3.2 Transition density functions

We are now ready to derive the transition density function of x_t defined by

$$f(y, x; t) \equiv \frac{d}{dx} P\{x_t \leq x | x_0 = y\}.$$

In order to calculate $f(y, x; t)$, we define the processes

$$x_t^H \equiv x_0 + \mu_H t + \sigma_L z_t, \quad x_t^L \equiv x_0 + \mu_L t + \sigma_L z_t.$$

Associated with these Brownian motions are

$$M_t \equiv \max_{s \leq t} x_s^H, \quad m_t \equiv \min_{s \leq t} x_s^L.$$

The process M_t represents the maximum of the process x_s^H up until time t , while m_t stands for the minimum of the process x_s^L before time t .

We also define the (joint) transition density functions

$$\begin{aligned} \ell_H(y, x; t) &\equiv \frac{d}{dx} P\{x_t^H \leq x, M_t < \bar{x} | x_0 = y\}, \\ \ell_L(y, x; t) &\equiv \frac{d}{dx} P\{x_t^L \leq x, m_t > \underline{x} | x_0 = y\}. \end{aligned}$$

It is well known (see, e.g., Harrison, 1985) that these functions are given by

$$\begin{aligned} \ell_H(y, x; t) &= \frac{1}{\sqrt{2\pi\sigma_H^2 t}} \exp\left\{-\frac{(x-y-\mu_H t)^2}{2\sigma_H^2 t}\right\} \\ &\quad - \frac{e^{\frac{2\mu_H}{\sigma_H^2}(\bar{x}-y)}}{\sqrt{2\pi\sigma_H^2 t}} \exp\left\{-\frac{(x+y-2\bar{x}-\mu_H t)^2}{2\sigma_H^2 t}\right\}, \quad x < \bar{x}, \end{aligned} \quad (3.10)$$

and

$$\begin{aligned} \ell_L(y, x; t) &= \frac{1}{\sqrt{2\pi\sigma_L^2 t}} \exp\left\{-\frac{(x-y-\mu_L t)^2}{2\sigma_L^2 t}\right\} \\ &\quad - \frac{e^{-\frac{2\mu_L}{\sigma_L^2}(y-\underline{x})}}{\sqrt{2\pi\sigma_L^2 t}} \exp\left\{-\frac{(x+y-2\underline{x}-\mu_L t)^2}{2\sigma_L^2 t}\right\}, \quad x < \underline{x}, \end{aligned} \quad (3.11)$$

respectively.

Proposition 3.1 *Suppose $S_{i0} = H$. Then, the transition density function is given by*

$$f(y, x; t) = \ell_H(y, x; t) + m_L * \ell_H(\underline{x}, x; \cdot)(t) + m_H * \ell_L(\bar{x}, x; \cdot)(t). \quad (3.12)$$

The other case is similar and given in Appendix A.4

Proof. See Appendices A.2 and A.4.

The Laplace transform of the transition density $f(y, x; t)$ with respect to t is given by

$$\begin{aligned}\mathcal{L}_t[f(y, x; \cdot)](\theta) &= \mathcal{L}_t[\ell_H(y, x; \cdot)](\theta) + \mathcal{L}_t[m_L](\theta)\mathcal{L}_t[\ell_H(\underline{x}, x; \cdot)](\theta) \\ &\quad + \mathcal{L}_t[m_H](\theta)\mathcal{L}_t[\ell_L(\bar{x}, x; \cdot)](\theta).\end{aligned}$$

Since the Laplace transforms in the right-hand side of the above equation are all derived in Appendix A.1, the transition density function can be calculated by the inverse Laplace transform as

$$\begin{aligned}f(y, x; t) &= \ell_H(y, x; t) + \mathcal{L}_\theta^{-1}\left[\mathcal{L}_t[m_L](\theta)\mathcal{L}_t[\ell_H(\underline{x}, x; \cdot)](\theta)\right](t) \\ &\quad + \mathcal{L}_\theta^{-1}\left[\mathcal{L}_t[m_H](\theta)\mathcal{L}_t[\ell_L(\bar{x}, x; \cdot)](\theta)\right](t),\end{aligned}\tag{3.13}$$

where \mathcal{L}_θ^{-1} stands for the inversion operator of the Laplace transform $\mathcal{L}_t[f](\theta)$ with respect to θ .

Although the transition density and the expectation of x_t cannot be obtained in closed form in general, the limiting density can be derived analytically, as the next proposition shows.

Proposition 3.2 *Suppose that $\mu_L < 0 < \mu_H$. Then, irrespective of the initial state, we have*

$$\lim_{t \rightarrow \infty} f(y, x; t) = \begin{cases} \frac{\exp\left\{\frac{2\mu_H}{\sigma_H^2}(x-\underline{x})\right\} - \exp\left\{\frac{2\mu_H}{\sigma_H^2}(x-\bar{x})\right\}}{\mu_H}, & -\infty < x < \underline{x}, \\ \frac{1 - \exp\left\{\frac{2\mu_H}{\sigma_H^2}(x-\bar{x})\right\}}{\mu_H} - \frac{1 - \exp\left\{\frac{2\mu_L}{\sigma_L^2}(x-\underline{x})\right\}}{\mu_L}, & \underline{x} \leq x \leq \bar{x}, \\ \frac{\exp\left\{\frac{2\mu_L}{\sigma_L^2}(x-\underline{x})\right\} - \exp\left\{\frac{2\mu_L}{\sigma_L^2}(x-\bar{x})\right\}}{\mu_L}, & \bar{x} < x \leq \infty, \end{cases}\tag{3.14}$$

and

$$\lim_{t \rightarrow \infty} E^y[x_t] = \frac{\bar{x} + \underline{x}}{2} + \frac{1}{2} \frac{\frac{\mu_L}{\mu_H} \sigma_H^2 - \frac{\mu_H}{\mu_L} \sigma_L^2}{\mu_H - \mu_L},\tag{3.15}$$

where $E^y[\cdot]$ is the conditional expectation operator under $x_0 = y$.

Proof. See Appendix A.3.

Note that the limiting density (3.14) is independent of the initial value y of the process x_t (and so is the limiting expectation). When $|\mu_H| = |\mu_L|$ and $\sigma_H = \sigma_L$, the limiting expectation (3.15) is equal to the middle point between \bar{x} and \underline{x} . How far the limiting expectation shifts from the middle point is determined by the second term of (3.15). For example, when σ_H is much larger than σ_L , the limiting expectation is closer to \underline{x} , and vice versa. On the other hand, a larger $|\mu_H|$ induces the limiting expectation closer to \bar{x} . These findings are consistent with our intuition.

3.3 A numerical example: Individual environmental policy

We first present the result of Monte Carlo simulation to illustrate how each policy maker chooses the environmental policy and how the level of environmental quality evolves over time. Figure 2 depicts the paths of the Monte Carlo simulation, where the parameter values are taken from Table 4 in the next section.

[Figure 2 is inserted here]

The initial level of pollution is set to be between the two thresholds, and the initial policy is assumed to be deregulation. As x_t first touches \bar{x} (i.e. at $t = T_{H1}$), the policy maker switches the policy to environmental regulation, and the log-level of pollution starts declining in average because of the tight regulation for the pollution. The policy maker alternately switches the policy afterwards.

It is observed from the numerical simulation that the policy maker in each area follows the so-called on-off strategy. Therefore, the realized path of environmental quality usually takes a form of oscillation between \bar{x}_i and \underline{x}_i .⁶ The log-level of pollution is usually going upward when a policy maker adopts deregulation policy, and it is decreasing otherwise. Note that the first switching time epochs $T_1 = T_{H1}$ in simulated paths are concentrated around $t = 20$, while the switching times T_n for $n = 2, 3, \dots$ are more dispersed.

Next, we calculate the density function $f(y, x; t)$ using the Laplace inversion formula (3.13). For this purpose, we invoke the numerical procedure proposed by Abate and Valkó (2004), which is known to be a very efficient method for the Laplace inversion. Figure 3 depicts an example of the transition density function $f(y, x; t)$, where the parameters are taken from Table 4.

[Figure 3 is inserted here]

In this example, the highest (most likelihood) point of the density function is changing in time, illustrating how the policy switching epoch is estimated. For example, the first hump appears around $t = 20$ and $x = 2$, that corresponds to T_{H1} . At this time epoch, the policy maker is most likely to change the policy from deregulation to regulation for the first time. We also observe some peaks, corresponding to T_{L1} , T_{H2} , and so on. However, as time goes by, the transition density function becomes flatter between \underline{x} and \bar{x} . This is because the probability law of x_t converges to the limiting distribution (stationary in time) when time goes to infinity.

⁶ Of course, because of uncertainty in the log-pollution level x_t , it often overshoots the switching levels.

4 The EKC: Λ shape or N shape?

The previous section considered an individual environmental policy, and found that the environmental quality exhibits an oscillation between upper and lower thresholds, i.e., not an inverted-U shape in a microeconomic setting, as far as each policy maker follows the optimal policy. However, as Arrow et al. (1995) mentioned, the EKC problem should be discussed in terms of the accumulation of local effects over long term periods. In this section, we consider an aggregated level of pollution in a macroeconomic setting and show that it exhibits either a Λ -shaped or an N -shaped pattern under some assumptions, even when each local area adopts the optimal on-off switching strategy.

This section starts by stating our assumptions explicitly, and then derives the *double* Laplace transform of the aggregated pollution level. The Laplace transform is easily inverted back to show that the pollution as a whole exhibits such patterns as Λ or N shapes.

4.1 The model in an aggregated level

Consider the situation that there are many local authorities in total who take charge of environmental policy and the influence of each authority is quite small. Suppose also that each authority executes its environmental policy myopically, meaning that cooperation among local authorities is not taken into consideration.⁷ In this situation, the assumption that the log-level of pollution in each local area follows a diffusion process can be justified, and the Brownian motions that drive uncertainty are considered to be mutually independent.

For each log-level x_{it} of pollution of area i , consider the weighted average

$$X_t = \sum_{i=1}^N w_i x_{it},$$

where $w_i > 0$ and $\sum_{i=1}^N w_i = 1$. Here, w_i represents the influence of area i relative to the aggregated level, and N is the number of local authorities all over the world. Also, $x_{i0} = y_i \equiv \log P_{i0}$ and, because economic scales of local authorities are different, the initial values y_i are distinct over local areas.

Under the above assumptions, when N is sufficiently large and each w_i is sufficiently

⁷ Cooperative policies among local authorities are of course an important factor for environmental problems. However, recall that the EKC issue has been discussed since early 1990s, and the discussion on the cooperative framework of global environmental protection started after that time. Hence, we need to show that the EKC is observed even when each local authorities behaves myopically toward environmental problems.

small, the effect from the law of large numbers (LLN) becomes dominant.⁸ Then, the expectation of X_t ,

$$E[X_t] = \sum_{i=1}^N w_i E^{y_i}[x_{it}],$$

is the only important statistics to be studied.

In order to investigate the function $h^{\text{EKC}}(t) \equiv E[X_t]$ with respect to time t , we consider the *double* Laplace transform of X_t . Define

$$\mathcal{L}_{t,x}[X](\theta, \xi) \equiv \int_0^\infty E[e^{-\xi X_t}] e^{-\theta t} dt.$$

It is readily seen that

$$\mathcal{L}_t[h^{\text{EKC}}](\theta) = - \left. \frac{\partial}{\partial \xi} \mathcal{L}_{t,x}[X](\theta, \xi) \right|_{\xi=0}. \quad (4.1)$$

The next result holds by linearity.

Proposition 4.1 *Under the assumptions stated above, we have*

$$\mathcal{L}_t[h^{\text{EKC}}](\theta) = - \sum_{i=1}^N w_i \left. \frac{\partial}{\partial \xi} \mathcal{L}_{t,x}[f_i(y_i, \cdot; \cdot)](\theta, \xi) \right|_{\xi=0}, \quad (4.2)$$

where $f_i(y, x; t)$ is the transition density function of area i given in (3.12).

By the definition of the double Laplace transform, we have

$$\begin{aligned} \mathcal{L}_{t,x}[f(y, \cdot; \cdot)](\theta, \xi) &= \int_{-\infty}^\infty e^{-\xi x} \left(\int_0^\infty e^{-\theta t} f(y, x; t) dt \right) dx \\ &= \int_{-\infty}^\infty e^{-\xi x} \mathcal{L}_t[f(y, x; t)](\theta) dx \\ &= \mathcal{L}_{t,x}[\ell_H(y, \cdot; \cdot)](\theta, \xi) + \mathcal{L}_t[m_L](\theta) \mathcal{L}_{t,x}[\ell_H(\bar{x}, \cdot; \cdot)](\theta, \xi) \\ &\quad + \mathcal{L}_t[m_H](\theta) \mathcal{L}_{t,x}[\ell_L(\bar{x}, \cdot; \cdot)](\theta, \xi). \end{aligned}$$

The double Laplace transforms of $\ell_H(y, x; t)$ and $\ell_L(y, x; t)$ are provided by (A.5) and (A.6), respectively, in Appendix A.1.

Using these results, simple but tedious algebra yields

$$\frac{\partial}{\partial \xi} \mathcal{L}_{t,x}[\ell_H(y, x; t)](\theta, 0) = e^{\frac{\mu_H}{\sigma_H^2}(\bar{x}-y)} \left(\frac{\bar{x}}{\theta} + \frac{\mu_H}{\theta^2} \right) e^{-\sqrt{\frac{\mu_H^2(\bar{x}-y)^2}{\sigma_H^4} + \frac{2(\bar{x}-y)^2}{\sigma_H^2}} \theta} - \left(\frac{y}{\theta} + \frac{\mu_H}{\theta^2} \right)$$

and

$$\frac{\partial}{\partial \xi} \mathcal{L}_{t,x}[\ell_L(y, x; t)](\theta, 0) = \left(\frac{\bar{x}}{\theta} + \frac{\mu_L}{\theta^2} \right) e^{-\frac{\mu_L + \sqrt{\mu_L^2 + 2\sigma_L^2 \theta}}{\sigma_L^2} (y-\bar{x})} - \left(\frac{y}{\theta} + \frac{\mu_L}{\theta^2} \right).$$

Substituting these results into (4.2), the Laplace transform $\mathcal{L}_t[h^{\text{EKC}}](\theta)$ is expressed in closed form. The inverse Laplace transform then calculates the expectation $h^{\text{EKC}}(t) \equiv E[X_t]$.

⁸ In fact, all we need in this discussion is to assume that the weak form of LLN holds true. Hence, the independence assumption can be removed if the total variance does not grow linearly in N .

4.2 A numerical example: Aggregated pollution level

This subsection provides a numerical example to show how the function $h^{\text{EKC}}(t)$ behaves in time t using Proposition 4.1 and the Laplace inversion technique.

According to Proposition 4.1, we need to specify parameters for all local authorities. However, in order to clarify how an environmental policy affects the pollution level and its dynamics, we make our numerical example as simple as possible, while keeping it realistic enough. To this end, we divide local authorities into two groups, depending on the current environmental policy, and assume that the model parameters are the same for all local areas except the initial states.⁹ This simplification may be justified in practice, when technological transfers are smoothly performed and each local authority owns environmental policy whose effectiveness is similar to all local areas. The difference of the initial states reflects that of current economic scales of the local authorities.

Let \mathcal{A}_H and \mathcal{A}_L be the sets of local areas whose current (time $t = 0$) environmental policies are deregulation and tight regulation, respectively, and assume that $\mu_k^i = \mu_k$, $\sigma_k^i = \sigma_k$, $c_i = c$ and $u_k^i = u_k$ for all i . Under the assumption, the switching thresholds \bar{x}_i and \underline{x}_i are the same for all local authorities, and the function $h^{\text{EKC}}(t)$ is expressed as

$$h^{\text{EKC}}(t) = \sum_{i \in \mathcal{A}_H} w_i E^{y_i} [x_{it}] + \sum_{i \in \mathcal{A}_L} w_i E^{y_i} [x_{it}]. \quad (4.3)$$

We denote the first and second terms of the right-hand side in (4.3) by $h^H(t)$ and $h^L(t)$, respectively, and assume

$$h^k(t) \approx w_k E^{y_k} [x_t]; \quad w_k \equiv \sum_{i \in \mathcal{A}_k} w_i, \quad y_k \equiv \sum_{i \in \mathcal{A}_k} w_i y_i, \quad k = H, L,$$

as a first approximation.¹⁰

4.2.1 A specific example: CO2 emission

In the following, we consider the dynamics of CO2 emission as our specific example. OECD countries and non-OECD countries are regarded as local areas whose current environmental policy is L and H , respectively. The reason why OECD countries are under tight regulation is that most of the OECD countries have ratified the Kyoto Protocol.¹¹

⁹ Of course, we can discuss more general cases. However, we find no significant qualitative difference through ample numerical experiments even when the parameters are set to be distinct over local areas.

¹⁰ Typically, local areas whose current environmental policies are deregulation are developing countries, while those under tight regulation are developed countries. This approximation may be justified, if the current economic scales of developed countries are similar and so are those of developing countries.

¹¹ Although the US has not yet ratified the Kyoto protocol, we regard the US as belonging to the regulated group, because the US has some regulation policies such as ‘America’s Climate Security Act of 2007’.

Table 4: The estimated parameters

	μ_k	σ_k	y_k	w_k
\mathcal{A}_L	-0.005	0.025	2.515	0.5
\mathcal{A}_H	0.043	0.052	0.132	0.5

4.2.2 Parameter estimation

We use the data for CO2 emission reported by Energy Information Administration¹² during 1980–2006. The UK and China are chosen as representative countries of \mathcal{A}_L and \mathcal{A}_H , respectively, and the parameters μ_k , σ_k and y_k for $k = L, H$ are estimated by the maximum likelihood method. The estimated parameters are listed in Table 4. As expected, the drift and volatility for \mathcal{A}_H are quite large compared to those for \mathcal{A}_L ; cf. Table 1.

On the other hand, for the weight parameter w_k , we use the environmental data compendium of the OECD, which shows that the emission amounts of OECD and non-OECD countries are almost the same, whence we set $w_H = w_L = 0.5$.

It remains to estimate the two thresholds \bar{x} and \underline{x} . However, the cost of policy implementation, as well as benefit and disutility from CO2 emission, seems hard to estimate from public data only. Hence, we calculate the function $h^{\text{EKC}}(t)$ with various values of the thresholds and analyze how the thresholds affect the shape of the curve.

4.2.3 Numerical results: Λ -shaped pattern

Figure 4 depicts the graph of the emission level with respect to time for the case that $\bar{x} = 2.0$ and $\underline{x} = 1.0$. The graph shows that the aggregated emission level exhibits a Λ -shaped pattern, meaning that the environmental degradation initially increases and then starts decreasing to converge to a certain level. However, this is a result of the sum of $h^H(t)$ and $h^L(t)$. Namely, from the graphs, it is observed that the curve $h^L(t)$ is always decreasing in time, while the curve $h^H(t)$ rapidly increases at an initial stage and then starts decreasing afterwards.

[Figure 4 is inserted here.]

The intuitive explanation of this result is as follows. When the current value x_{i0} , $i \in \mathcal{A}_H$, of emission level is low, a policy maker takes a deregulation policy to expand their economic

¹² The data is available on their website <http://www.eia.doe.gov/emeu/international/carbondioxide.html>.

scales, and the emission level increases rapidly at an early stage, as for most of the non-OECD countries. However, once the environmental degradation touches the upper threshold, the policy maker will switch its policy to regulation, so that the emission level starts decreasing on average. The time epochs for policy switches vary, depending on how x_{it} evolves in time, over the countries belonging to \mathcal{A}_H . That is, the realized switching times T_{kn}^i may differ among local areas, although they are identically distributed. In particular, the switching times T_{kn}^i for $n = 2, 3, \dots$ become dispersed more and more. Accumulation of these dispersed realizations will cancel each other due to the weak LLN, and the pollution level converges to the mean of the stationary distribution.

On the other hand, OECD countries have already experienced economic development and adopt regulation policies for their environment. That is, the current value x_{i0} , $i \in \mathcal{A}_L$, of emission level is high, and a tight regulation policy is taken currently. In this case, the emission level monotonically decreases on average, thanks to the weak LLN, even though some countries may adopt a deregulation policy in future for the purpose of economic growth.

Finally, the emission level as a whole shows a Λ -shaped curve, because the increase of emission level for countries in \mathcal{A}_H has a dominant impact for the aggregation at an early stage, and afterwards both curves converge to the limiting expectation monotonically.

4.2.4 Numerical results: N -shaped pattern

The story becomes different when the two thresholds for the policy switch are distant. Figure 5 shows the graph of the emission level with respect to time for the case that $\bar{x} = 2.5$ and $\underline{x} = 1.0$, while Figure 6 depicts the graph when $\bar{x} = 2.0$ and $\underline{x} = 0.5$. In these cases, the aggregated level of emission exhibits an N -shaped pattern as reported in some empirical researches (e.g., de Bruyn and Opschoor, 1997; Sengupta, 1997), meaning that the aggregated emission level will start again increasing after a certain period of time to converge.

[Figures 5 and 6 are inserted here.]

From the graphs in these figures, it is observed that not only the curve $h^H(t)$ but also $h^L(t)$ show a U -shaped hump. The reason is as follows. When the two thresholds for the policy switch are distant, it takes time to reach the lower threshold. This implies that the duration for the first policy becomes longer for each country in \mathcal{A}_L and, due to the weak LLN, the first switching times T_{L1}^i from regulation to deregulation are rather concentrated at some point of time. This is the reason why the U -shaped hump is observed in $h^L(t)$. Recall that this mechanism is the same as the one that the inverted- U -shaped hump appears for $h^H(t)$ in an early stage. The reason for the U -shaped hump in $h^H(t)$ is similar.

4.2.5 Some discussions

Note that the thresholds for policy switch are mainly determined by the cost of policy implementations. More specifically, when the cost of policy implementation is high (low, respectively), the option value for the policy switch is low (high) and each policy maker has less (more) incentive to change the policy. Hence, from the above results, an N -shaped pattern is more likely observed for the pollution level when the cost of policy implementation is relatively high,¹³ while a Λ -shaped pattern will appear when the cost is relatively low.

Finally, it is worth mentioning that the EKC usually refers to the relationship between the pollution level and the per capita GDP, while this paper shows a pattern of either N or Λ shapes with respect to *time*.¹⁴ However, the per capita GDP also grows in average exponentially in time. Since accumulation of pollutant is a by-product of economic activities, the assumption of a GBM pollution with varying coefficient is justifiable, and the EKC of pollution with per capita GDP also holds in our setting. Moreover, the EKC curve with respect to time is more useful when it is applied for policy problems in practice.

5 Concluding Remarks

In this paper, we propose a simple (switching) real options model to explain why the environmental Kuznets curve (EKC) appears for various pollutants when each policy maker optimally executes its environmental policy. The key idea is that the switching dynamics of environmental policy is described by an alternating renewal process. The double Laplace transform of transition density of a pollutant level is obtained by a novel application of renewal theory. The expected level of overall pollutants is then calculated numerically and found to exhibit either a Λ -shaped or an N -shaped pattern in time.

Although a realized path of pollution level in each local area shows an oscillation, the pollution in an aggregated level shows an EKC if each policy maker myopically adopts an optimal policy. This is because all local authorities are generous to pollution at an early stage, but tight regulation is chosen as the level of pollution becomes high enough. Since the subsequent policy shifts after the first switch varies among areas, depending on the realized path of pollution, the aggregated level first increases and then starts decreasing to converge to a certain limiting mean due to the law of large numbers. The environmental

¹³ This result is consistent with Dinda (2004), which claims that pollutant for which the end-of-pipe solution is costly may follow an N -shaped pattern.

¹⁴ Lopez and Mitra (2000) consider the EKC with respect to a growth factor, which can be regarded as time.

degradation follows an EKC under a fairly general setup, implying that the effect of policy implementations is an important factor for the dynamics of environmental quality in an economy with uncertainty and irreversibility.

Our model provides theoretically one possible explanation for the EKC observed in the actual world. In particular, our model is more flexible than the existing models to be able to produce both Λ and N -shapes, recently reported in many empirical researches, depending on the cost of policy implementations. Our finding indicates that when uncertainty and irreversibility are taken into account, effects of policy implementation are of great importance for the dynamics of environmental quality.

It should be noted that, applying the results in Shiryaev (1978), the geometric Brownian motion (GBM) assumption on the pollutant level can be generalized to a Markov process with different regimes. That is, if the level of pollution is continuous and its drift and volatility satisfy some smooth conditions such as Hölder continuity, then the optimal policy includes two constant thresholds, although it is difficult to determine the thresholds even numerically, and the policy takes the form that the policy switching occurs when the level of pollution touches the thresholds. This implies that, when a policy maker executes environmental policy optimally (or nearly optimally in practice), the pollution level of each area oscillates over time and an aggregated level shows an EKC in a more general setup.

As a future work, our model can be applied to predict when the peak of the EKC will present, if all the parameters in our model are estimated from the actual data. Such empirical studies are important, since we are able to propose a more realistic and feasible policy toward environmental problems.

A Appendix

This Appendix provide explicit formulas of the Laplace transforms, necessary for the development of our analyses, and the proofs of propositions.

A.1 Laplace transform formulas

Here, we provide explicit formulas of the Laplace transforms of interest in this paper.¹⁵

First, since we have f_{0H} , f_L and f_H as in (3.3)–(3.5), direct calculation yields

$$\mathcal{L}_t[f_{0H}](\theta) = \exp \left\{ -\frac{\bar{x} - x_0}{\sigma_H^2} \left(\sqrt{\mu_H^2 + 2\sigma_H^2\theta} - \mu_H \right) \right\},$$

¹⁵ Detailed derivations of the Laplace transforms are available from authors upon request.

$$\begin{aligned}\mathcal{L}_t[f_L](\theta) &= \exp\left\{-\frac{\bar{x}-\underline{x}}{\sigma_L^2}\left(\sqrt{\mu_L^2+2\sigma_L^2\theta}+\mu_L\right)\right\}, \\ \mathcal{L}_t[f_H](\theta) &= \exp\left\{-\frac{\bar{x}-\underline{x}}{\sigma_H^2}\left(\sqrt{\mu_H^2+2\sigma_H^2\theta}-\mu_H\right)\right\}.\end{aligned}$$

It follows from (3.8) and (3.9) that

$$\mathcal{L}_t[m_H](\theta) = \frac{e^{-\frac{\bar{x}-y}{\sigma_H^2}\left(\sqrt{\mu_H^2+2\sigma_H^2\theta}-\mu_H\right)}}{e^{\frac{\bar{x}-x}{\sigma_H^2}\left(\sqrt{\mu_H^2+2\sigma_H^2\theta}-\mu_H\right)} - e^{-\frac{\bar{x}-x}{\sigma_L^2}\left(\sqrt{\mu_L^2+2\sigma_L^2\theta}+\mu_L\right)}} \quad (\text{A.1})$$

and

$$\mathcal{L}_t[m_L](\theta) = \frac{e^{-\frac{\bar{x}-y}{\sigma_H^2}\left(\sqrt{\mu_H^2+2\sigma_H^2\theta}-\mu_H\right)}}{e^{\frac{\bar{x}-x}{\sigma_L^2}\left(\sqrt{\mu_L^2+2\sigma_L^2\theta}+\mu_L\right)} - e^{-\frac{\bar{x}-x}{\sigma_H^2}\left(\sqrt{\mu_H^2+2\sigma_H^2\theta}-\mu_H\right)}}, \quad (\text{A.2})$$

respectively.

Next, from (3.10) and (3.11), similar calculation yields

$$\mathcal{L}_t[\ell_H](\theta) = \begin{cases} \frac{e^{\frac{\mu_H+\sqrt{\mu_H^2+2\sigma_H^2\theta}}{\sigma_H^2}(x-y)} - e^{\frac{\mu_H+\sqrt{\mu_H^2+2\sigma_H^2\theta}}{\sigma_H^2}(x-\bar{x}) + \frac{\mu_H-\sqrt{\mu_H^2+2\sigma_H^2\theta}}{\sigma_H^2}(\bar{x}-y)}}{\sqrt{\mu_H^2+2\sigma_H^2\theta}}, & x < y, \\ \frac{e^{\frac{\mu_H-\sqrt{\mu_H^2+2\sigma_H^2\theta}}{\sigma_H^2}(x-y)} - e^{\frac{\mu_H+\sqrt{\mu_H^2+2\sigma_H^2\theta}}{\sigma_H^2}(x-\bar{x}) + \frac{\mu_H-\sqrt{\mu_H^2+2\sigma_H^2\theta}}{\sigma_H^2}(\bar{x}-y)}}{\sqrt{\mu_H^2+2\sigma_H^2\theta}}, & y \leq x \leq \bar{x}, \\ 0, & \bar{x} < x, \end{cases} \quad (\text{A.3})$$

and

$$\mathcal{L}_t[\ell_L](\theta) = \begin{cases} 0, & x < \underline{x}, \\ \frac{e^{\frac{\mu_L+\sqrt{\mu_L^2+2\sigma_L^2\theta}}{\sigma_L^2}(x-y)} - e^{\frac{\mu_L-\sqrt{\mu_L^2+2\sigma_L^2\theta}}{\sigma_L^2}(x-\underline{x}) - \frac{\mu_L+\sqrt{\mu_L^2+2\sigma_L^2\theta}}{\sigma_L^2}(y-x)}}{\sqrt{\mu_L^2+2\sigma_L^2\theta}}, & \underline{x} \leq x \leq y, \\ \frac{e^{\frac{\mu_L-\sqrt{\mu_L^2+2\sigma_L^2\theta}}{\sigma_L^2}(x-y)} - e^{\frac{\mu_L-\sqrt{\mu_L^2+2\sigma_L^2\theta}}{\sigma_L^2}(x-\underline{x}) - \frac{\mu_L+\sqrt{\mu_L^2+2\sigma_L^2\theta}}{\sigma_L^2}(y-x)}}{\sqrt{\mu_L^2+2\sigma_L^2\theta}}, & y < x, \end{cases} \quad (\text{A.4})$$

respectively.

Finally, from (3.10) and (3.11), the double Laplace transforms of $\ell_H(y, x; t)$ and $\ell_L(y, x; t)$ with respect to t and x are obtained as

$$\mathcal{L}_{t,x}[\ell_H](\theta, \xi) = \frac{2\left(e^{\frac{\mu_H-\sqrt{\mu_H^2+2\sigma_H^2\theta}}{\sigma_H^2}(\bar{x}-y)-\xi\bar{x}} - e^{-\xi y}\right)}{\sigma_H^2\xi^2 - 2\mu_H\xi - 2\theta} \quad (\text{A.5})$$

and

$$\mathcal{L}_{t,x}[\ell_L](\theta, \xi) = \frac{2 \left(e^{-\frac{\mu_L + \sqrt{\mu_L^2 + 2\sigma_L^2 \theta}}{\sigma_L^2} (y-x) - \xi x} - e^{-\xi y} \right)}{\sigma_L^2 \xi^2 - 2\mu_L \xi - 2\theta}, \quad (\text{A.6})$$

respectively.

A.2 Proof of Proposition 3.1

Consider the following three cases:

Case 1	$T_{H1} > t$
Case 2	$T_{H1} \leq t, S_t = L$
Case 3	$T_{H1} \leq t, S_t = H$

Note that these events are mutually exclusive and exhaust all the events. Associated with the cases are the following conditional density functions:

$$\begin{aligned} g_1(y, x; t) &\equiv \frac{d}{dx} P\{x_t \leq x | x_0 = y, T_{H1} > t\}, \\ g_2(y, x; t) &\equiv \frac{d}{dx} P\{x_t \leq x | x_0 = y, T_{H1} \leq t, S_t = L\}, \\ g_3(y, x; t) &\equiv \frac{d}{dx} P\{x_t \leq x | x_0 = y, T_{H1} \leq t, S_t = H\}, \end{aligned}$$

respectively. We calculate the conditional density functions using the key observation (3.7).

First, by definition, the function g_1 is equal to $\ell_H(y, x; t)$. For g_2 , note that

$$\{T_{H1} \leq t, S_t = L\} = \{N_H(t) \geq 1, N_H(t) - N_L(t) = 1\}.$$

Since the event that the process $x_t = x_t^L$ hits \underline{x} at some time t occurs with the density $m_L(t)$, we have

$$g_2(y, x; t) = \int_0^t m_L(s) \ell_H(\underline{x}, x; t-s) ds.$$

Similarly, the fact $\{T_{H1} \leq t, S_t = L\} = \{N_H(t) \geq 1, N_H(t) - N_L(t) = 0\}$ yields

$$g_3(y, x; t) = \int_0^t m_H(s) \ell_L(\bar{x}, x; t-s) ds.$$

Therefore, combining these results, we get

$$\begin{aligned} f(y, x; t) &= g_1(y, x; t) + g_2(y, x; t) + g_3(y, x; t) \\ &= \ell_H(y, x; t) + m_L * \ell_H(\underline{x}, x; \cdot)(t) + m_H * \ell_L(\bar{x}, x; \cdot)(t), \end{aligned}$$

completing the proof of Proposition 3.1.

A.3 Proof of Proposition 3.2

It is well known that

$$\lim_{t \rightarrow \infty} m_k(t) = \lim_{\theta \downarrow 0} \theta \mathcal{L}_t[m_k(t)](\theta) = \frac{1}{E[\tau_L] + E[\tau_H]}, \quad k = H, L,$$

where $E[\tau_L] = E[\tau_{L_n}]$, $n = 1, 2, \dots$, and $E[\tau_H] = E[\tau_{H_n}]$, $n = 2, 3, \dots$. Hence, from (3.12), the limiting density is given by

$$\lim_{t \rightarrow \infty} f(y, x; t) = \frac{1}{E[\tau_L] + E[\tau_H]} \int_0^\infty [\ell_H(\underline{x}, x; t) + \ell_L(\bar{x}, x; t)] dt,$$

irrespective of the initial state. From (3.10) and (3.11), direct calculation yields

$$\int_0^\infty \ell_H(\underline{x}, x; t) dt = \begin{cases} \frac{e^{\frac{2\mu_H}{\sigma_H^2}(x-\underline{x})} - e^{\frac{2\mu_H}{\sigma_H^2}(x-\bar{x})}}{\mu_H}, & -\infty < x < \underline{x}, \\ \frac{1 - e^{\frac{2\mu_H}{\sigma_H^2}(x-\bar{x})}}{\mu_H}, & \underline{x} \leq x \leq \bar{x}, \\ 0, & \bar{x} < x < \infty, \end{cases}$$

and

$$\int_0^\infty \ell_L(\bar{x}, x; t) dt = \begin{cases} 0, & -\infty < x < \underline{x}, \\ \frac{e^{\frac{2\mu_L}{\sigma_L^2}(x-\underline{x})} - 1}{\mu_L}, & \underline{x} \leq x \leq \bar{x}, \\ \frac{e^{\frac{2\mu_L}{\sigma_L^2}(x-\underline{x})} - e^{\frac{2\mu_L}{\sigma_L^2}(x-\bar{x})}}{\mu_L}, & \bar{x} < x \leq \infty, \end{cases}$$

respectively. (3.14) now follows at once. (3.15) is obtained by direct calculation.

A.4 Results for the case of $S_{i0} = L$

When $S_{i0} = L$, the density functions are given by the following:

Interarrival time	Density function
τ_{L1}	$f_{0L}(t)$
$\tau_{Hn}; n = 2, 3, \dots$	$f_H(t)$
$\tau_{Ln}; n = 2, 3, \dots$	$f_L(t)$

Here,

$$f_{0L}(t) = \frac{x_0 - \underline{x}}{\sigma_L \sqrt{2\pi t^3}} \exp \left\{ -\frac{(x_0 - \underline{x} + \mu_L t)^2}{2\sigma_L^2 t} \right\},$$

and $f_H(t)$ and $f_L(t)$ are the same as (3.4) and (3.5), respectively. It follows from the basic renewal theory that the Laplace transforms of m_L and m_H are derived as

$$\mathcal{L}_t[m_L] = \frac{\mathcal{L}_t[f_{0L}](\theta)}{1 - \mathcal{L}_t[f_H](\theta)\mathcal{L}_t[f_L](\theta)}, \quad (\text{A.7})$$

$$\mathcal{L}_t[m_H] = \frac{\mathcal{L}_t[f_{0L}](\theta)\mathcal{L}_t[f_H](\theta)}{1 - \mathcal{L}_t[f_H](\theta)\mathcal{L}_t[f_L](\theta)}, \quad (\text{A.8})$$

respectively. Also, by similar discussions as for Proposition 3.1, we obtain the transition density function as

$$\begin{aligned} f(y, x; t) &= \ell_L(y, x; t) + m_H * \ell_L(\underline{x}, x; \cdot)(t) + m_L * \ell_H(\bar{x}, x; \cdot)(t) \\ &= \ell_L(y, x; t) + \mathcal{L}_\theta^{-1} \left[\mathcal{L}_t[m_H](\theta)\mathcal{L}_t[\ell_L(\underline{x}, x; \cdot)](\theta) \right](t) \\ &\quad + \mathcal{L}_\theta^{-1} \left[\mathcal{L}_t[m_L](\theta)\mathcal{L}_t[\ell_H(\bar{x}, x; \cdot)](\theta) \right](t). \end{aligned} \quad (\text{A.9})$$

As in Proposition 4.1, the expectation $h^{EKC}(t) = E[X_t]$ can be calculated numerically via the double Laplace transform of (A.9).

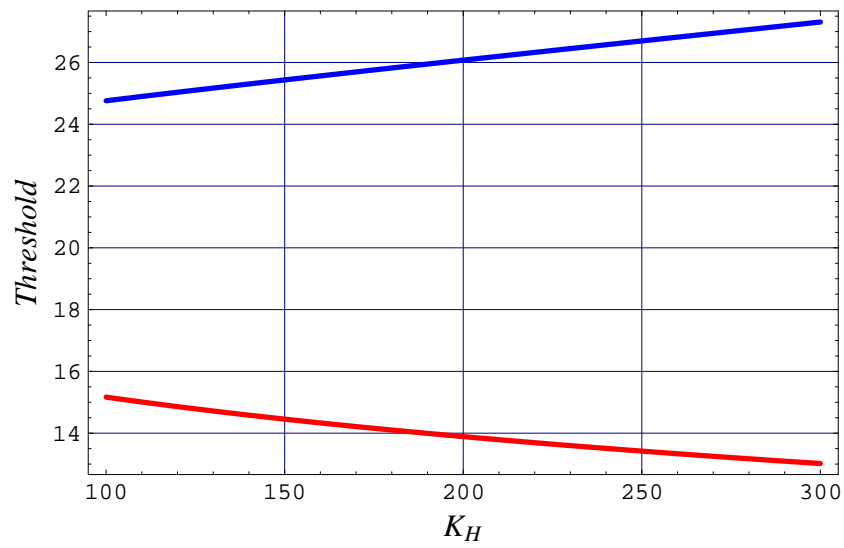
References

- Abate, J. and P.P. Valkó (2004), “Multi-Precision of Laplace Transform Inversion,” *International Journal for Numerical Methods in Engineering*, **60**, 979–993.
- Andreoni, J. and A. Levinson (2001), “The Simple Analytics of the Environmental Kuznets Curve,” *Journal of Public Economics*, **80**, 269–286.
- Arrow, K., B. Bolin, R. Constanza, P. Dasgupta, C. Folke, C. Holling, B.-O. Jansson, S. Levin, K.-G. Mäler, C. Perrings, and D. Pimentel (1995), “Economic Growth, Carrying Capacity and the Environment,” *Ecological Economics*, **15**, 91–95.
- Brock, W.A. and M.S. Taylor (2004), “The Green Solow Model,” NBER Working Paper No.10557.
- de Bruyn, S.M. and J.B. Opschoor (1997), “Developments in the Throughput–Income Relationship: Theoretical and Empirical Observations,” *Ecological Economics*, **20**, 255–268.
- Dinda, S. (2004), “Environmental Kuznets Curve Hypothesis: A Survey,” *Ecological Economics*, **49**, 431–455.
- Dixit, A.K. and R.S. Pindyck (1994), *Investment under Uncertainty*, Princeton University Press.

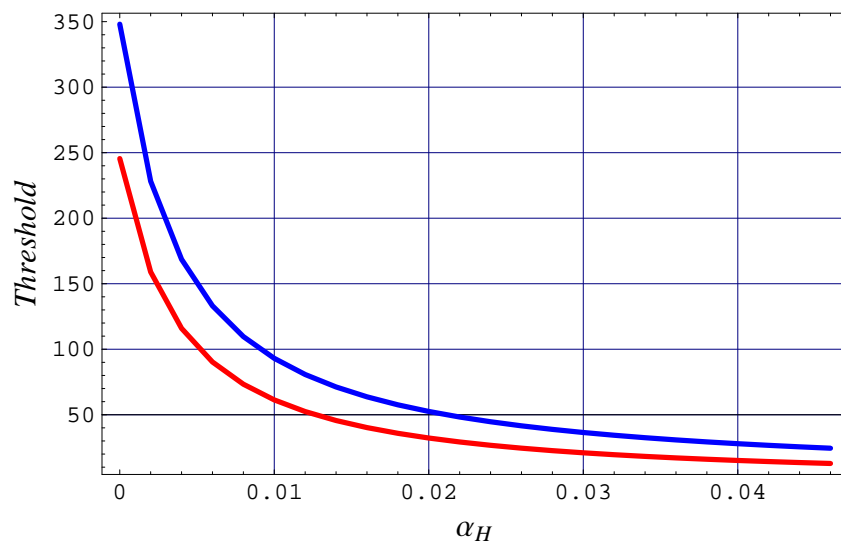
- Grossman, G.M. and A.B. Krueger (1995), “Economic Growth and the Environment,” *Quarterly Journal of Economics*, **110**, 353–377.
- Jones, L.E. and R.E. Manuelli (2000), “Endogenous Policy Choice: The Case of Pollution and Growth,” *Review of Economic Dynamics*, **4**, 369–405.
- Harrison, J.M. (1985), *Brownian Motion and Stochastic Flow Systems*, John Wiley and Sons.
- Kijima, M. (1997), *Markov Processes for Stochastic Modeling*, Chapman & Hall, London.
- Kijima, M., K. Nishide, and A. Ohyama (2009), “Economic Models for Environmental Kuznets Curve: A Survey,” working paper.
- Kuznets, S. “Economic Growth and Income Inequality,” *American Economic Review*, **45**, 1–28.
- Lopez, R. (1994), “The Environment as a Factor of Production: The Effects of Economic Growth and Trade Liberalization,” *Journal of Environmental Economics and Management*, **27**, 163–184.
- Lopez, R. and S. Mitra (2000), “Corruption, Pollution, and the Kuznets Environmental Curve,” *Journal of Environmental Economics and Management*, **40**, 137–150.
- Magnani, E. (2001), “The Environmental Kuznets Curve: Development Path or Policy Result?” *Environmental Modelling and Software*, **16**, 157–165.
- Michailidis A. and K. Mattas (2007), “Using Real Options Theory to Dam Investment Analysis: An Application of Binomial Option Pricing Model,” *Water Resources Management*, **21**, 1717–1733.
- Nishide, K. and A. Ohyama (2009), “Using Real Options Theory to a Country’s Environmental Policy: Considering the Economic Size and Growth,” *Operational Research: An International Journal*, to appear.
- Pindyck, R.S. (2000), “Irreversibilities and the Timing of Environmental Policy,” *Resource and Energy Economics*, **22**, 233–259.
- Pindyck, R.S. (2002), “Optimal Timing Problems in Environmental Economics,” *Journal of Economic Dynamics and Control*, **26**, 1677–1697.
- Pindyck, R.S. (2006), “Uncertainty in Environmental Economics,” *Review of Environmental Economics and Policy*, **1**, 45–65.

- Ross, S.M. (1983), *Stochastic Processes*, Wiley.
- Selden, T.M. and D. Song (1995), “Neoclassical Growth, the J Curve for Abatement and the Inverted U curve for Pollution,” *Journal of Environmental Economics and Management*, **29**, 162–168.
- Sengupta, R.P. (1997), “CO2 Emission–Income Relationship: Policy Approach for Climate Control,” *Pacific Asia Journal of Energy*, **7**, 207–229.
- Shiryaev, A.N. (1978), *Optimal Stopping Rules*, Springer.
- Stokey, N.L. (1998), “Are There Limits to Growth?” *International Economic Review*, **39**, 1–31.
- Wirl, F. (2006), “Pollution Thresholds under Uncertainty,” *Environment and Development Economics*, **11**, 493–506.

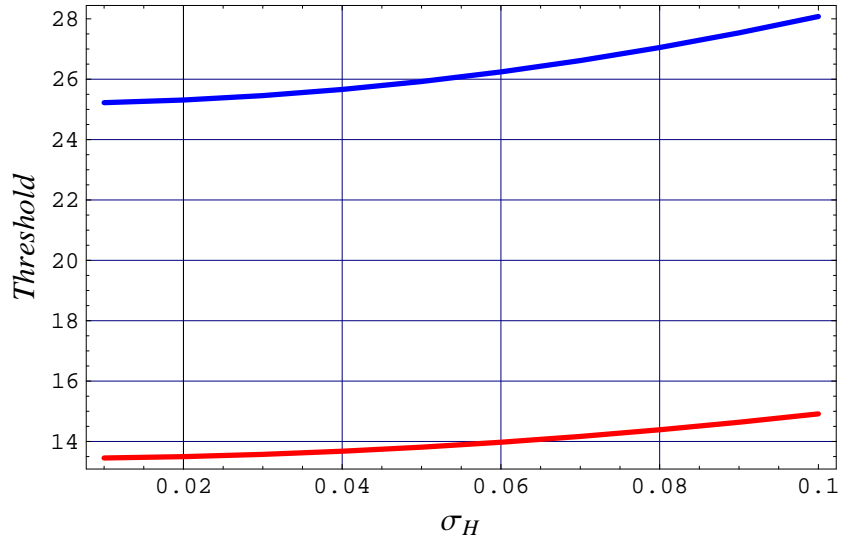
Figures



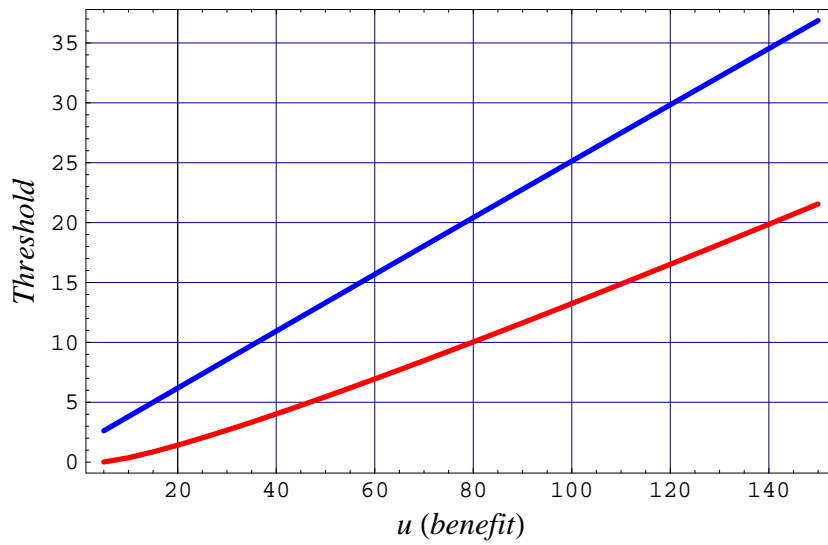
(a) Dependence of K_H^i on the thresholds



(b) Dependence of α_{iH} on the thresholds



(c) Dependence of σ_{iH} on the thresholds



(d) Dependence of u_H^i on the thresholds

Figure 1: Comparative static analysis: The effect on the thresholds \bar{P}_i and \underline{P}_i .

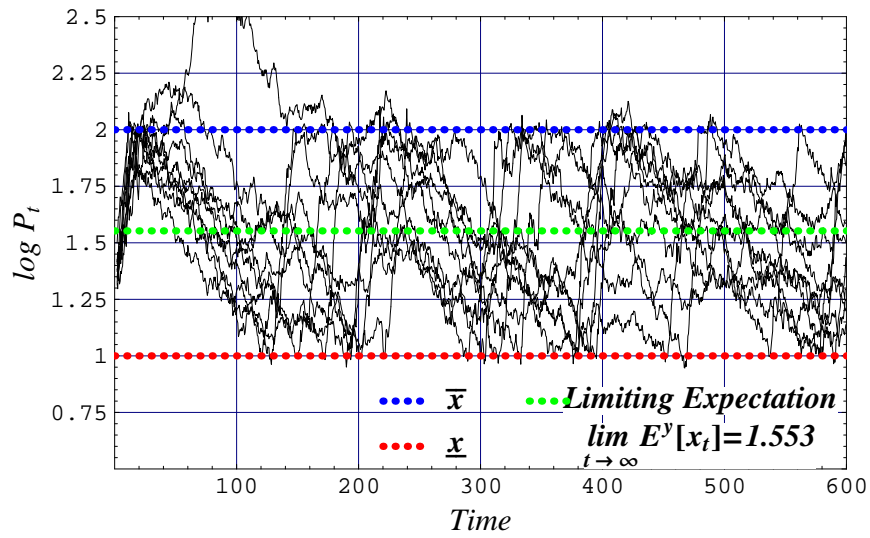


Figure 2: The result of Monte Carlo simulations. The parameter values are the same as in Table 2

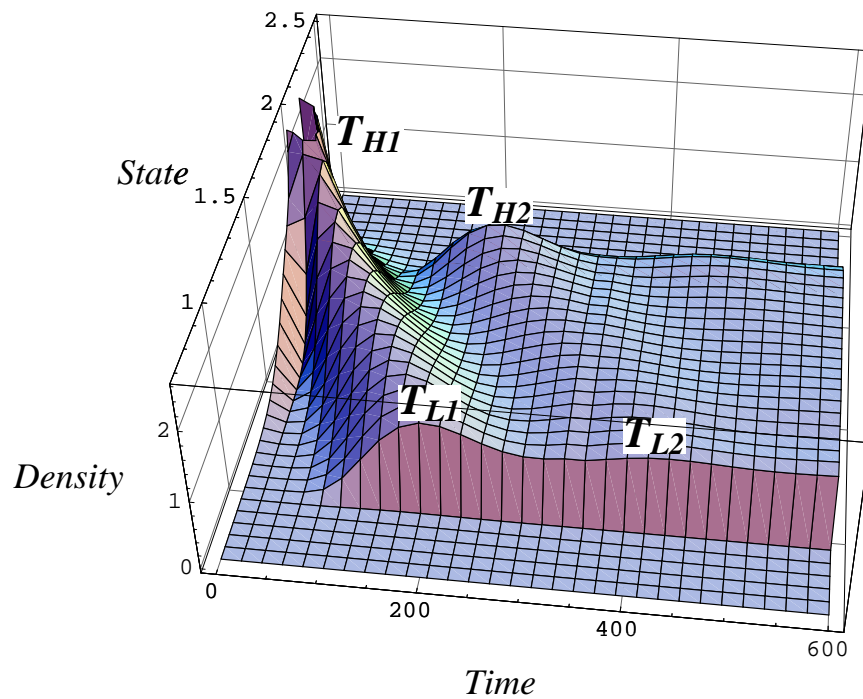


Figure 3: Transition density function. The parameters are $\mu_H = 0.043$, $\sigma_H = 0.052$, $\mu_L = -0.005$, $\sigma_L = 0.025$, $\bar{x} = 2$, $\underline{x} = 1$, and $x_0 = 1.3235$.

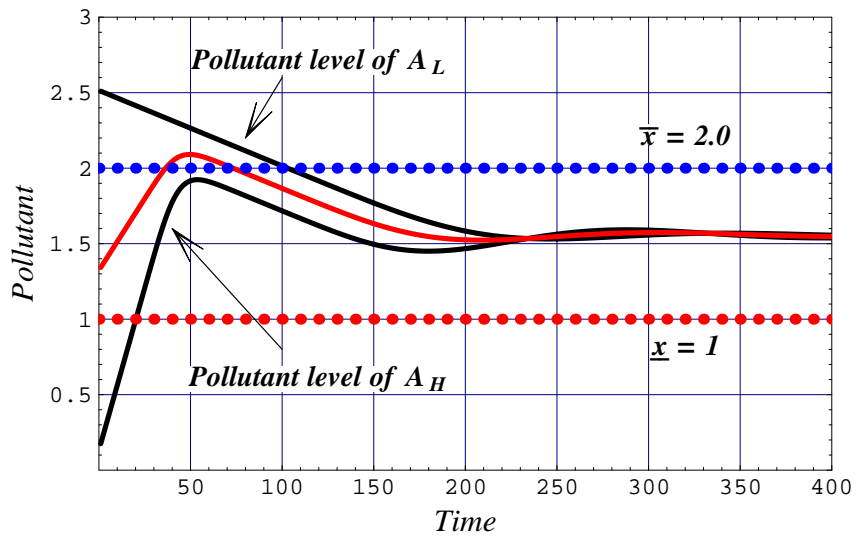


Figure 4: Dynamics of environmental quality for $\bar{x} = 2.0$ and $\underline{x} = 1.0$.

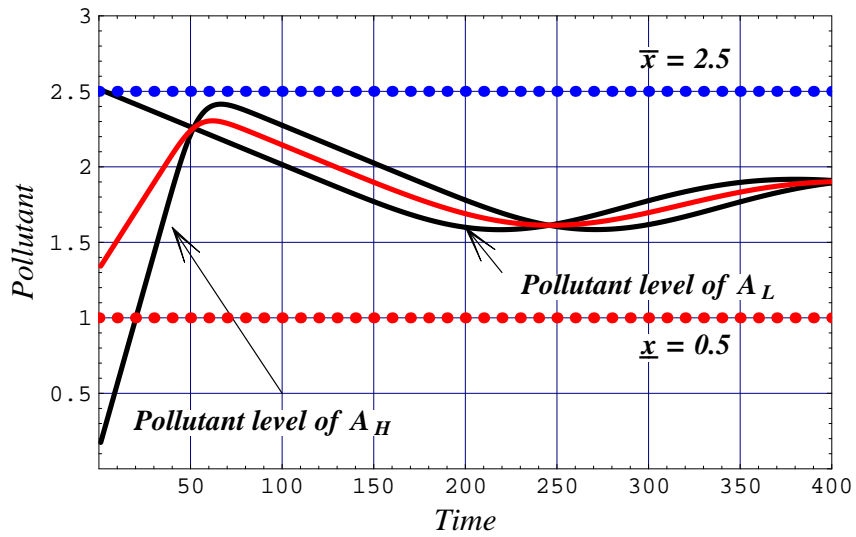


Figure 5: Dynamics of environmental quality for $\bar{x} = 2.5$ and $\underline{x} = 1.0$.

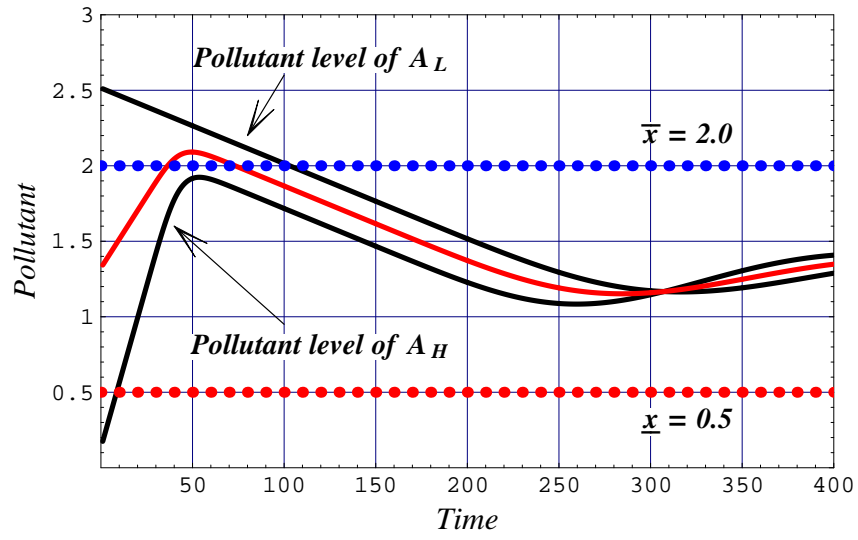


Figure 6: Dynamics of environmental quality for $\bar{x} = 2.0$ and $\underline{x} = 0.5$.